

Structural Flexibility and Sorption Properties of 2D Porous Coordination Polymers Constructed from Trinuclear Heterometallic Pivalates and 4,4'-Bipyridine

Ruslan A. Polunin,^[a] Sergey V. Kolotilov,^[a] Mikhail A. Kiskin,^[b] Olivier Cador,^[c] Stéphane Golhen,^[c] Oleksiy V. Shvets,^[a] Lahcène Ouahab,^{*,[c]} Zhanna V. Dobrokhotova,^[b] Victor I. Ovcharenko,^[d] Igor L. Eremenko,^{*,[b]} Vladimir M. Novotortsev,^[b] and Vitaly V. Pavlishchuk^{*,[a]}

Keywords: Polymers / Porous materials / Adsorption / Structural flexibility / Hydrophobic interactions / Solvent effects

The temperature dependence of crystal structure parameters of isostructural coordination polymers $\text{Fe}_2\text{MO}(\text{Piv})_6(\text{bipy})_{1.5} \cdot 2\text{DMF}$ [**1**·2DMF and **2**·2DMF, where $\text{M} = \text{Ni}^{\text{II}}$ or Co^{II} , respectively, $\text{Piv} = (\text{CH}_3)_3\text{CCO}_2^-$, $\text{bipy} = 4,4\text{-bipyridine}$ and DMF is N,N -dimethylformamide] was studied at five temperatures in the range from 120 to 296 K. The X-ray structure of the N,N -diethylformamide (DEF) solvate of the same coordination polymer **1**, $\text{Fe}_2\text{NiO}(\text{Piv})_6(\text{bipy})_{1.5} \cdot 2\text{DEF}$ (**1**·2DEF), was studied at 173 and 260 K. Both the DMF and DEF solvates possess similar crystal structures, consisting of a series of parallel 2D polymeric layers with honeycomb voids. These series of parallel layers intersect, leading to their interpenetration and formation of zig-zag channels. It was found that the change of temperature and/or solvent molecule in the pores causes significant structural rearrangement associated with a change of the separation between parallel layers and the angle between intersecting layers. These structural changes

lead to a variation of the calculated solvent-accessible volume from $0.21 \text{ cm}^3 \text{ g}^{-1}$ (120 K, **2**·2DMF) to $0.30 \text{ cm}^3 \text{ g}^{-1}$ (260 K, **1**·2DEF) for a probe molecule with $r = 1.4 \text{ \AA}$. These changes can model structural transformations which can occur at desolvation and adsorption of guests. Adsorption of n -hexane, n -octane, methanol and ethanol by $\text{Fe}_2\text{MO}(\text{Piv})_6(\text{bipy})_{1.5}$ was studied. The sorption isotherms of alkanes were typical for microporous sorbents and in this case the behaviour of the coordination polymers resembled that which is typical for sorbents with a rigid structure. In a contrast, alcohol sorption capacity continuously grew at increasing pressure which may be caused by structural transformations, similar to temperature-induced structural transformations. Among the studied sorbates, sorption capacity grew in order methanol < ethanol < n -hexane < n -octane which may be caused by the hydrophobic nature of the channels (due to the presence of *tert*-butyl groups).

Introduction

Interest in porous coordination polymers and metal-organic frameworks has been invoked by their high sorption

capacity in terms of different substrates^[1] in combination with other physical properties, such as nontrivial magnetic behaviour,^[2] luminescence,^[3] conductivity^[4] etc. as well as chemical properties such as catalytic activity.^[5] Many MOFs possess “rigid” structures, meaning that their crystal lattice does not change significantly during adsorption or desorption of substrates of differing natures (such as gases, water, organic compounds, etc.).^[6] However, there are a lot of examples of so-called “breathing polymers”, i.e. MOFs, which undergo structural transformations upon inclusion or liberation of guest molecules.^[7] Such compounds can possess new properties which cannot be achieved in the case of the sorbents of other classes, for example, the gate-opening phenomenon.^[8] Though the mechanism of structural rearrangement is sometimes clear,^[7a,7b] in many cases such processes may involve unexpected changes in the crystal lattice, especially when the structural elements of the MOF are not linked by covalent bonds in 3D. However, determination of the crystal structure of the coordination polymer after removal of solvent and/or adsorption of substrate is usually impossible due to severe lattice disorder or even

[a] L. V. Pisarzhevskii Institute of Physical Chemistry of the National Academy of Sciences of the Ukraine, Prospekt Nauki 31, Kiev 03028, Ukraine
Fax: +38-44-5256216
E-mail: shchuk@inphyschem-nas.kiev.ua

[b] N. S. Kurnakov Institute of General and Inorganic Chemistry, Russian Academy of Sciences, Leninsky Pros. 31, 119991 Moscow, GSP-1, Russian Federation
Fax: +7-495-9541279
E-mail: ilerem@igic.ras.ru

[c] Equipe Organométalliques et Matériaux Moléculaires, Sciences Chimiques de Rennes, UMR UR1-CNRS 6226, Université de Rennes 1, Campus de Beaulieu, 35042 Rennes cedex, France
Fax: +33-2-23236840
E-mail: ouahab@univ-rennes1.fr

[d] International Tomography Centre, Siberian Branch, Russian Academy of Sciences, Institutskaya str. 3a, 630090 Novosibirsk, Russian Federation
Fax: +7-383-3331399
E-mail: Victor.Ovcharenko@tomo.nsc.ru

Supporting information for this article is available on the WWW under <http://dx.doi.org/10.1002/ejic.201100791> or from the author.

complete collapse of single crystals. Understanding the so-called “structural rearrangements” processes, invoked by desolvation or resolution, is one of the important tasks of modern physical-inorganic and materials chemistry.

Recently we reported two new isostructural MOFs, built from trinuclear heterometallic pivalates $\text{Fe}_2\text{MO}(\text{Piv})_6(\text{bipy})_{1.5}\cdot 2\text{DMF}$ [$\text{M} = \text{Ni}^{\text{II}}$, compound **1**·2DMF, or Co^{II} , compound **2**·2DMF, $\text{Piv} = (\text{CH}_3)_3\text{CCO}_2^-$, $\text{bipy} = 4,4$ -bipyridine and DMF is N,N -dimethylformamide].^[9] It was shown that these complexes, in unsolvated forms, could adsorb N_2 and H_2 . Unusual hysteresis of nitrogen adsorption-desorption was found and as possible reasons we proposed some steric hindrances for N_2 molecules passing deeply into the channels or “gate-opening” which could involve changes in the crystal packing of the coordination polymers.

The aim of this work was to study the peculiarities of structural flexibility of the compounds $\text{Fe}_2\text{MO}(\text{Piv})_6(\text{bipy})_{1.5}$ which could be responsible for the above-mentioned gate-opening and to study sorption properties of these compounds in terms of a wide range of adsorbate molecules.

Compounds $\text{Fe}_2\text{MO}(\text{Piv})_6(\text{bipy})_{1.5}$ can be considered as suitable models for obtaining information about the flexibility of crystal structures of 2D coordination polymers. Single crystals of these MOFs retain sufficiently good quality for single-crystal X-ray structure determination at various temperatures, despite noticeable changes in the unit cell parameters and mutual orientation of the 2D polymeric layers. Hence, examination of the compounds $\text{Fe}_2\text{MO}(\text{Piv})_6(\text{bipy})_{1.5}\cdot\text{Solv}$ at different temperatures can enable estimation of the range in which the structural parameters of these compounds can vary. Quantitative information about possible structural changes in these compounds is important for understanding their sorption properties, especially adsorption of substrates which may cause some structural transformations.

In this paper we report the variation in the crystal structures of $\text{Fe}_2\text{MO}(\text{Piv})_6(\text{bipy})_{1.5}\cdot\text{Solv}$ induced by change of solvent ($\text{Solv} = \text{DMF}$ or DEF , where $\text{DEF} = N,N$ -diethylformamide) and/or temperature (from 120 to 296 K). These results illustrate the flexibility of crystal structures and a modification of the characteristics in their voids. Differential scanning calorimetry (DSC) measurements were performed in order to obtain information about possible phase changes. The range of adsorbates was extended to alkanes and alcohols (compared with previously studied N_2 and H_2)^[9] which enabled the identification of significant differences between sorption of adsorbates of different classes which may be associated with structural flexibility of the MOF as well as the hydrophobic nature of their pores.

Results and Discussion

Temperature- and Solvent-Induced Structural Variation of **1**·2Solv and **2**·2Solv

Since the crystal structures of compounds **1**·2DMF and **2**·2DMF at 150 and 120 K, respectively, were reported by

us previously only a brief description of important features is provided here. The structures of **1**·2DMF were determined by using the data collected at three temperatures between 160 and 296 K and a previous experiment performed at 150 K^[9] was used to analyse structural variations over a wide temperature range (Table 1). In addition, the X-ray structures of **2**·2DMF (at 120 K)^[9] as well as those of **1**·2DEF at 173 and 260 K were analysed to provide additional information about the possible range of crystal structure changes.

Table 1. Selected structural parameters of **1**·2DMF and **2**·2DMF (compounds are isostructural) at different temperatures.

T/K	$d/\text{\AA}^{[a]}$	$\Phi/^\circ$	Volume of voids/ cm^3g^{-1} [b]
DMF solvates			
120	10.800(5)	63.56(1)	0.21
150	10.849(5)	64.38(1)	0.22
160	10.930(5)	65.36(1)	0.22
260	11.242(8)	68.525(7)	0.27
296	11.277(4)	69.208(9)	0.27
DEF solvates			
173	11.357(5)	71.51(5)	0.28
260	11.447(5)	72.290(7)	0.30

[a] d and ϕ are defined in the text, also see part b of Figure 1. [b] Calculated by using PLATON for a probe molecule with $r = 1.4\text{ \AA}$. The crystal density was taken from the crystallographic data (for the case when there is no solvent in voids). For more details see Figure 2.

Compounds **1**·2DMF and **2**·2DMF are isostructural and crystallise in the monoclinic system (space group $P2_1/n$). Since no difference was found between the structures of **1**·2DMF and **2**·2DMF at the same temperature, we decided to merge the two compounds in our study. Two DMF molecules per formula unit of **1** and **2** were found, though in the majority of cases (especially at “high” temperatures) these DMF molecules could not be reliably localised because of disorder and were removed by the SQUEEZE procedure.

As we previously reported,^[9] the crystal structures of **1** and **2** are built from interpenetrating 2D layers with a pseudo-honeycomb topology (Figure 1, a). Each 2D layer is formed by trinuclear μ_3 -oxocentered $\text{Fe}_2\text{CoO}(\text{Piv})_6$ units connected by bipy molecules. The solvate with DEF, namely **1**·2DEF, is also built from very similar 2D layers of a honeycomb shape with the same type of interpenetration and it generally has the same topology as the DMF solvate (Figure 1, b) despite the two existing in different crystal systems (orthorhombic vs. monoclinic). The type of solvate molecule does not influence the topology of the coordination polymer $\text{Fe}_2\text{MO}(\text{Piv})_6(\text{bipy})_{1.5}$ but leads to a change of structural parameters such as the mutual orientation of 2D layers, as will be shown below. The channels in the polymers $\text{Fe}_2\text{MO}(\text{Piv})_6(\text{bipy})_{1.5}$ have the shape of a periodic zig-zag along the b axis (in DMF solvates) or along the a axis (in DEF solvates).

The temperature variation in the range from 260 to 120 K led to a continuous change of the unit cell parameters (Table 1 and Figure S1, Supporting materials). In par-

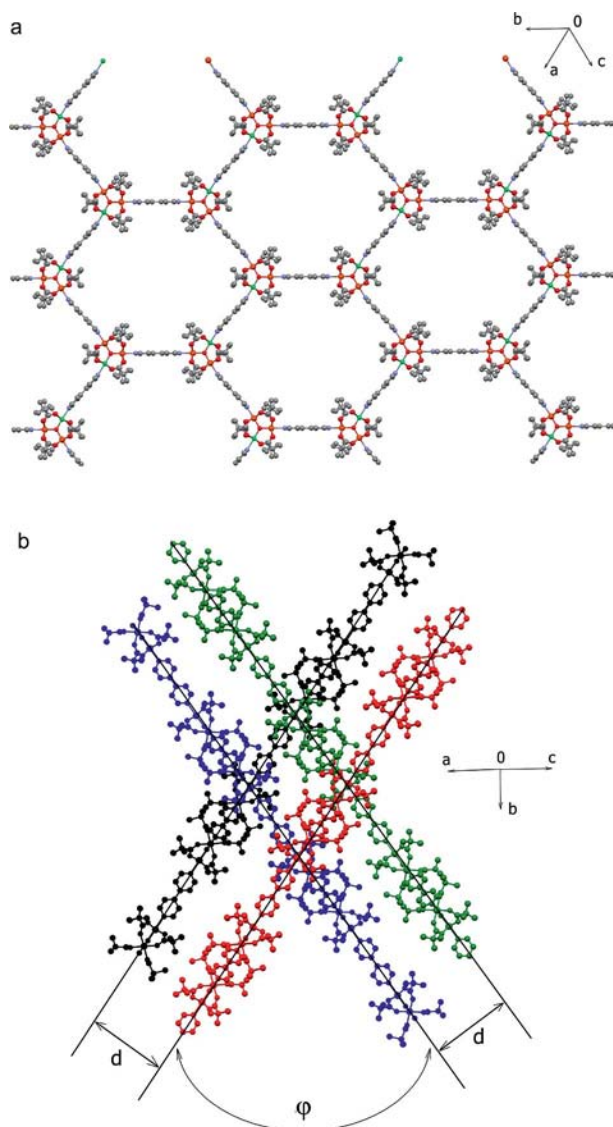


Figure 1. **a**: One 2D layer in 1·2DMF at 260 K, **b**: mutual orientation of such layers in the crystal. Hydrogen atoms are omitted for clarity. Schemes for other solvates or at other temperatures are visually the same (except different d and ϕ , see text). The orientation of the crystallographic axes, shown on this figure, is valid only for the $P2_1/n$ space group.

ticular, β monotonously decreased from $95.72(1)^\circ$ to $91.755(1)^\circ$ with the temperature decreasing. Notably, these structural changes are completely reversible which was confirmed by a unit cell measurement of the same single crystal of 1·2DMF at several temperatures, including heating after being cooled.

For the purposes of a structural description, each layer can be represented by a plane passing through six μ_3 -O atoms of six $\text{Fe}_2\text{MO}^{6+}$ units in a distorted hexagon $\{\text{Fe}_2\text{MO}(\text{Piv})_6\}_6\{\text{bipy}\}_6$ (Figure 1, a). The deviations of the metal ions from these planes are negligibly small so that these planes can be considered to be those containing all metal ions in each hexagon $\{\text{Fe}_2\text{MO}(\text{Piv})_6\}_6\{\text{bipy}\}_6$. In the cases of the DMF solvates (space group $P2_1/n$), the above mentioned planes coincide with the crystallographic planes

(-222) and equivalent planes for one set of parallel 2D layers as well as the $(11\bar{1})$ and equivalent planes for another set of parallel 2D layers. For 1·2DEF (space group $Pbca$) these planes coincide with the (-102) crystallographic planes and equivalent planes and the (204) and equivalent planes for two sets of parallel layers. The distortion of each hexagon within a 2D layer can be characterised by its “diagonals” (l , the distances between opposite μ_3 -O atoms in the hexagon) and the angles between the “edges” of the hexagon (θ , being the angles between the lines passing through μ_3 -O atoms of three consequent neighbouring $\text{Fe}_2\text{MO}^{6+}$ units) while the crystal structure of the polymer can be characterised by the separation between the neighbouring parallel planes (d) and the angle between the intersecting planes (ϕ , Figure 1, b).

The temperature change in the range between 120 and 296 K has no influence on the parameters of each separate 2D layer in 1·2DMF and 2·2DMF such as the $\text{M}\cdots\text{M}$ separations within Fe_2MO units, the $\text{M}\cdots\text{M}$ separations between the bipy bridge or l and θ (as defined above) (Table S2, Supporting materials). However, a temperature change in the same range results in noticeable variation in the separations between adjacent planes (d) and the angles ϕ between intersecting 2D layers [when T drops from 296 to 120 K, d decreases from 11.277(4) to 10.800(5) Å, while ϕ decreases from $69.208(9)$ to $63.56(1)^\circ$, Table 1].

Compared with the DMF solvate, 1·2DEF is characterised by larger separations between the 2D grid [the d value for 1·2DEF even at 173 K is larger than this for 1·2DMF at 296 K, i.e. 11.357(5) vs. 11.277(4) Å] and a larger angle ϕ [$71.51(5)$ vs. $69.208(9)^\circ$, respectively]. These changes are consistent with the size of the solvent molecules: the larger DEF molecule occupies more space compared with the smaller DMF molecule and causes more significant “expansion” of the structure.

Finally, from the analysis of the crystal structures of the DMF and DEF solvates it can be concluded that due to a change in the solvent and/or temperature, d can vary from 10.800(5) Å to 11.447(5) Å, and ϕ from $63.56(1)^\circ$ to $72.290(7)^\circ$ (Table 1). Calculations performed with PLATON^[10] for a $r = 1.4$ Å probe showed significant variations of the solvent-accessible volume ranging from 22.4% to 29.8% (this corresponds to 0.21 cm³ g^{−1} and 0.30 cm³ g^{−1}, respectively, Figure 2) depending on the solvent in the voids and/or temperature. These changes are associated with apparent changes of the appearances of the channels: the increase of free volume is associated with a decreasing of zig-zag period and an increase in the pore diameter (Figure 3).

In one of the attempts to collect data for a single crystal of 1·2DMF in the monoclinic crystal system at room temperature, the unit cell parameter β varied from $96.48(3)^\circ$ (at the beginning of the experiment) to $94.86(9)^\circ$ (10 min from the beginning of data collection) and to $91.61(1)^\circ$ (120 min from the beginning of data collection). These values are consistent with the tendency of β to change with T . Thus, solvent loss leads to a change in the mutual orientation of the 2D layers (associated with a decrease in the volume of the voids) which similar to that observed on decreasing the

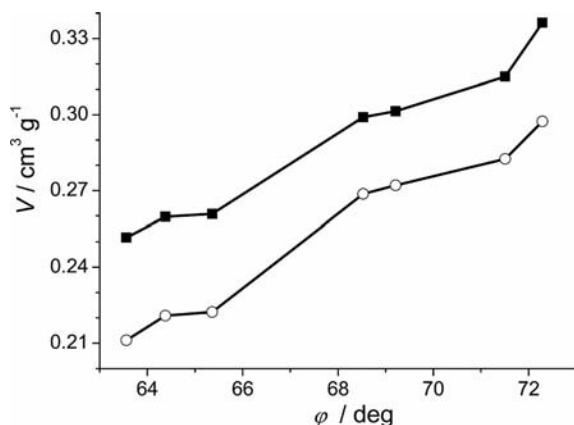


Figure 2. Change in the calculated volumes of the voids in **1** and **2** depending on ϕ for a probe molecule with $r = 1.2 \text{ \AA}$ (■) and 1.4 \AA (○). Solid lines are to guide the eye.

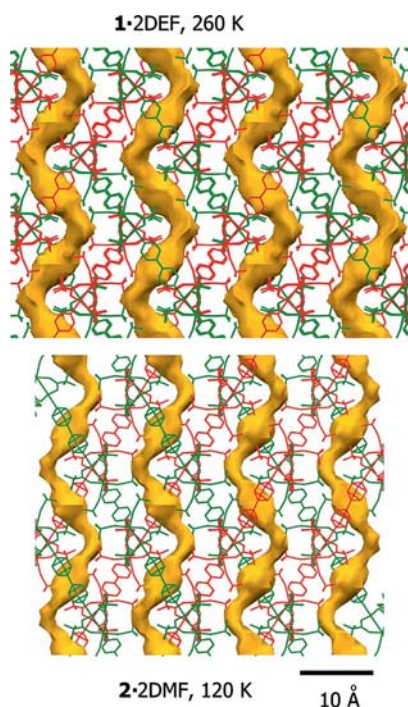


Figure 3. The appearances of the channels in the polymers $\text{Fe}_2\text{MO}(\text{Piv})_6(\text{bipy})_{1.5} \cdot 2\text{Solv}$, which correspond to the largest volume in the top ($M = \text{Ni}$, $\text{Solv} = \text{DEF}$, at $T = 260 \text{ K}$) and the lowest volume in the bottom ($M = \text{Co}$, $\text{Solv} = \text{DMF}$, at $T = 120 \text{ K}$) among the studied X-ray structures. Mercury diagram for probe molecule with $r = 1.4 \text{ \AA}$.

temperature. Other unit cell parameters, obtained in this experiment, are presented in the Supporting Information (Table S3).

We have shown that due to the flexibilities of the crystal structures of $\text{Fe}_2\text{MO}(\text{Piv})_6(\text{bipy})_{1.5} \cdot 2\text{Solv}$, the solvent accessible volume in these compounds may decrease by 1.4 times depending on the temperature and the nature of solvent molecules in the voids, according to PLATON estimation. Complexes $\text{Fe}_2\text{MO}(\text{Piv})_6(\text{bipy})_{1.5}$ are examples of po-

rous coordination polymers, the structural flexibilities of which are associated with rearrangement of the mutual orientation of the polymeric layers in contrast to the variation of the angles in the coordination spheres of the metal ions.^[7c,7f] A thorough study of the thermal dependencies of the crystal structures of these polymers gives some understanding of the changes in the crystal structures which occur upon desolvation.

Differential Scanning Calorimetry Measurements

In order to get additional information about possible structural transformations of **1** with temperature, differential scanning calorimetry (DSC) measurements were performed on **1**·2DMF. On cooling, the compound undergoes an exothermic process between 160 and 140 K (which seems to consist of two consequential processes) with a total heat effect $-5.83(5) \text{ J g}^{-1}$ ($6.84 \text{ kJ} \cdot \text{mol}^{-1}$, Figure 4, a). A corresponding counter-process on heating occurs in the range from 150 to 165 K and the heat effect is $5.63(5) \text{ J g}^{-1}$ ($6.60 \text{ kJ} \cdot \text{mol}^{-1}$). These processes can probably be attributed to DMF rearrangement in the voids because the changes in

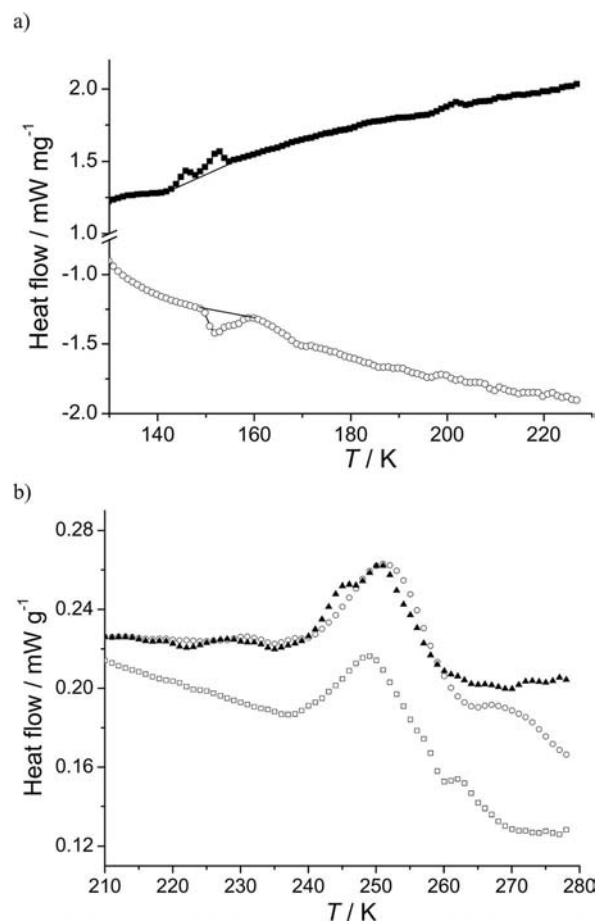


Figure 4. DSC curves for (a) the solvated compound **1**·2DMF, cooling (■) and heating (○), and (b) solvent-free **1** (three measurements of 3 different samples). Solid lines on the graphs (a) are to guide the eye.

all the unit cell parameters with temperature is monotonous (Figure S2, Supporting materials) and a solvent-free sample shows completely different behaviour.

DSC measurements for a solvent-free sample of **1** in the range from 295 to 173 K revealed an exothermic process at 263–238 K with a heat effect $-7.85(5) \text{ J g}^{-1}$ (8.1 kJ mol^{-1}). However no counter-process was detected during the heating process of the same sample. Repeated cooling of the same sample showed no process. This effect is probably associated with release of some structural tension which could occur during desolvation of the compound.

Thermal Behaviour and Powder X-ray Diffraction

The thermal behaviour of the solvent-free coordination polymers **1** and **2**, desolvated in vacuo, was determined by TG analysis and was found to be very similar for both. For example, during heating, compound **2** slowly loses weight from between ca. 40 °C to ca. 225 °C (Figure S3, Supporting Information). The weight loss was found to be equal to 2.7% at 100 °C, 4.5% at 120 °C reaching 15% at only 225 °C which may correspond to release of one bipy per formula unit (theor. weight loss is 15.2%). Upon further heating the weight loss slightly increases reaching 18.5% at 265 °C followed by abrupt increase. At 450 °C decomposition is complete (weight loss is 75%, which may correspond to CoFe_2O_4 , theor. weight loss is 77%^[11]).

The powder X-ray diffraction pattern of **1**·2DMF is consistent with the powder XRD pattern calculated from the data of X-ray structure of this compound at room temperature (Figure S4). Removal of DMF from the voids of **1**·2DMF leads to some structural rearrangement, as evidenced by X-ray powder analysis (Figure S4) and this was also confirmed by single-crystal X-ray measurements (vide supra).

Notably, there is significant difference between the XRD patterns, calculated for the same compound (**1**·2DMF) at 296 and 120 K. Thus, caution should be observed if powder XRD data, measured at room temperature, are compared with the pattern calculated from the X-ray structure determined from the data collected at low temperature.

Desolvation of compound **2** does not lead to a significant change in the powder X-ray diffraction pattern of this compound (Figure S5) and this may be associated with incomplete removal of DMF from the pores. This agrees with the result of N_2 and H_2 sorption measurements of samples **1** and **2** which showed considerably lower sorption capacities for **2** than for **1** in the case of N_2 and H_2 sorption.^[9] However, residual solvent can not be detected in **2** (as well as in **1**) by CHN analysis. It could be that few DMF molecules block the long channel and “fix” 2D layers, preventing their rearrangement. This supposition is consistent with the results of alkane or alcohol sorption whereby both **1** and **2** showed comparable capacity (vide infra). These substrates, probably, can “shift” residual DMF in pores at 293 K and occupy their total volume (vide infra). In any case, compound **1** can be considered as completely desolvated.

Sorption Properties

As was previously reported, compounds **1** and **2** (desolvated **1**·2DMF and **2**·2DMF) exhibit permanent porosity which was confirmed by sorption of nitrogen and hydrogen.^[9] The values of the surface S_{BET} were $520 \text{ m}^2 \cdot \text{g}^{-1}$ for **1** and $273 \text{ m}^2 \cdot \text{g}^{-1}$ for **2**, and the values of the pore volumes were $0.22 \text{ cm}^3 \cdot \text{g}^{-1}$ for **1** and $0.11 \text{ cm}^3 \cdot \text{g}^{-1}$ for **2** (from N_2 adsorption isotherms at 78 K). These characteristics of a porous structure are quite typical for microporous samples, except broad adsorption-desorption hysteresis, which was found in the case of nitrogen sorption. In order to get additional characteristics of the pores in **1** and **2**, sorption of additional organic substrates (*n*-hexane, *n*-octane, methanol and ethanol) was studied.

Isotherms of *n*-hexane adsorption by **1** and **2** are typical for microporous sorbents (isotherm of type I according to BDDT classification^[12]). Pores are already filled at $P \cdot P_s^{-1}$ of approximately 0.1 and a further increase of P does not lead to significant growth of the sorption volume until high pressures at which point inter-particle condensation begins (Figure 5, a, and Figure S6). There is negligible hysteresis on the *n*-hexane adsorption and desorption isotherms, suggesting the absence of some specific interactions between the coordination polymers with *n*-hexane or conformational

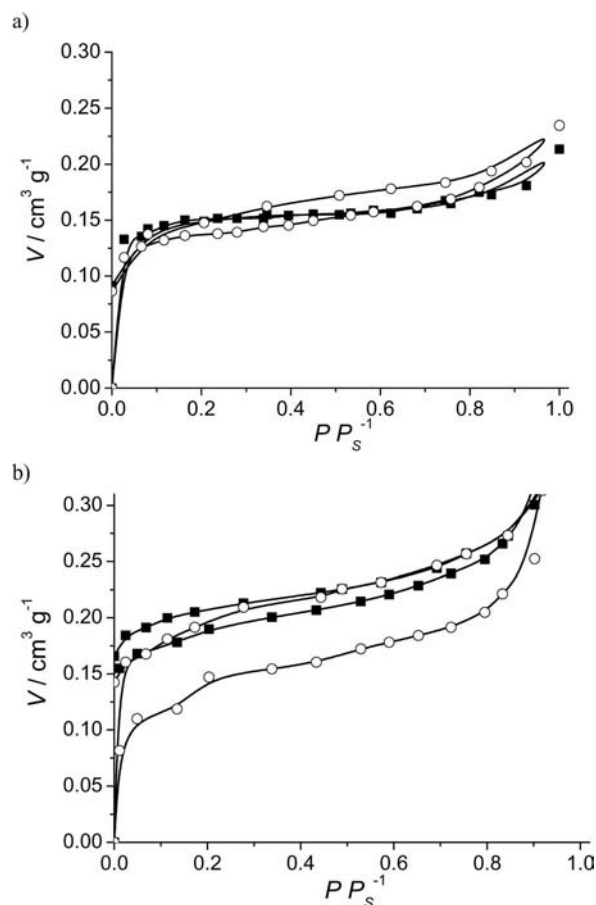


Figure 5. Isotherms of *n*-hexane (a) and *n*-octane (b) sorption by **1** (■) and **2** (○) at 293 K.

changes in the crystal structure of the polymer. From the *n*-hexane adsorption, S_{BET} was calculated to be $300 \text{ m}^2 \cdot \text{g}^{-1}$ for **1** and $280 \text{ m}^2 \cdot \text{g}^{-1}$ for **2**. The values of the pore volumes, calculated using the Dubinin-Radushkevich model, are $0.155(1) \text{ cm}^3 \cdot \text{g}^{-1}$ for **1** and $0.148(1) \text{ cm}^3 \cdot \text{g}^{-1}$ for **2**. In the case of **1** both S_{BET} and V_{pores} are lower than the corresponding values, determined from N_2 sorption, which is consistent with the larger size of the *n*-hexane molecule compared with N_2 . At the same time, in the case of **2**, S_{BET} and V_{pores} are slightly higher than the values, determined from N_2 sorption, which confirms the supposition that the channels in **2** could be partially blocked by residual DMF which was forced to move under the pressure of *n*-hexane. The characteristic adsorption energies E_a of *n*-hexane sorption, estimated using the Dubinin-Radushkevich model, are $21(1) \text{ kJ mol}^{-1}$ and $17(1) \text{ kJ mol}^{-1}$ for **1** and **2**, respectively (at 293 K). These values are about 1.5 times higher than the E_a of N_2 adsorption at 77 K [$12.0(5)$ and $13.6(5) \text{ kJ mol}^{-1}$ for **1** and **2**, respectively] and about 5 times higher than the E_a of H_2 adsorption at 77 K (3.1 and 3.2 kJ mol^{-1} for **1** and **2**, respectively).

The isotherms of *n*-octane sorption are generally similar to the case of *n*-hexane – there is rapid growth of the isotherms at low P (Figure 5, b, and Figure S6), and already at $P \cdot P_s^{-1} = 0.1$ sorption capacity reaches $0.17 \text{ cm}^3 \cdot \text{g}^{-1}$ for **1** and $0.11 \text{ cm}^3 \cdot \text{g}^{-1}$ for **2**, which is comparable with V_{pores} determined by *n*-hexane sorption. However, in contrast to *n*-hexane sorption, further increases in pressure led to noticeable growth of the volume of the adsorbed *n*-octane and at $P \cdot P_s^{-1} = 0.8$, the sorption capacity increased to $0.25 \text{ cm}^3 \cdot \text{g}^{-1}$ for **1** and $0.21 \text{ cm}^3 \cdot \text{g}^{-1}$ for **2**. The fitting of the low-pressure part of the adsorption isotherms ($P \cdot P_s^{-1} < 0.5$) by using the Dubinin-Radushkevich model gave $V_{\text{pores}} = 0.204(5) \text{ cm}^3 \cdot \text{g}^{-1}$ for **1** and $0.162(6) \text{ cm}^3 \cdot \text{g}^{-1}$ for **2** [characteristic adsorption energies E_a are $19(2)$ and $12(1) \text{ kJ mol}^{-1}$, respectively]. Similar to the cases of N_2 , H_2 and *n*-hexane sorption, the values of V_{pores} for **1** are higher than for **2** although there was wide hysteresis of *n*-octane sorption in the case of **2** and the *n*-octane desorption curve for **2** was very close to the sorption and desorption isotherms for **1** (Figure 5, b).

The sorption isotherms of methanol and ethanol (Figure 6 and Figure S7) were completely different from those found for *n*-hexane and *n*-octane. In the case of methanol no rapid growth in the adsorption isotherm, which could be expected for micropores filling, was observed and, in the case of ethanol, the isotherms grew to ca. $0.05 \text{ cm}^3 \cdot \text{g}^{-1}$ and $0.03 \text{ cm}^3 \cdot \text{g}^{-1}$ at $P \cdot P_s^{-1} = 0.03$ for **1** and **2**, respectively. With increasing pressure the sorption capacity more or less monotonously increased, reaching $0.21 \text{ cm}^3 \cdot \text{g}^{-1}$ and $0.19 \text{ cm}^3 \cdot \text{g}^{-1}$ (at $P \cdot P_s^{-1} = 0.97$) in the case of methanol or $0.27 \text{ cm}^3 \cdot \text{g}^{-1}$ and $0.25 \text{ cm}^3 \cdot \text{g}^{-1}$ (at $P \cdot P_s^{-1} = 1$) in the case of ethanol for **1** and **2**, respectively. More pronounced hysteresis on ethanol sorption isotherms compared with the isotherms of alkanes or methanol sorption may allow us to suppose that the energy of ethanol interaction with structural elements of **1** and **2** is the highest among these substrates. However, the E_a values of alcohol adsorption by **1**

and **2** can not be estimated because these isotherms are different from those expected for classical microporous samples.

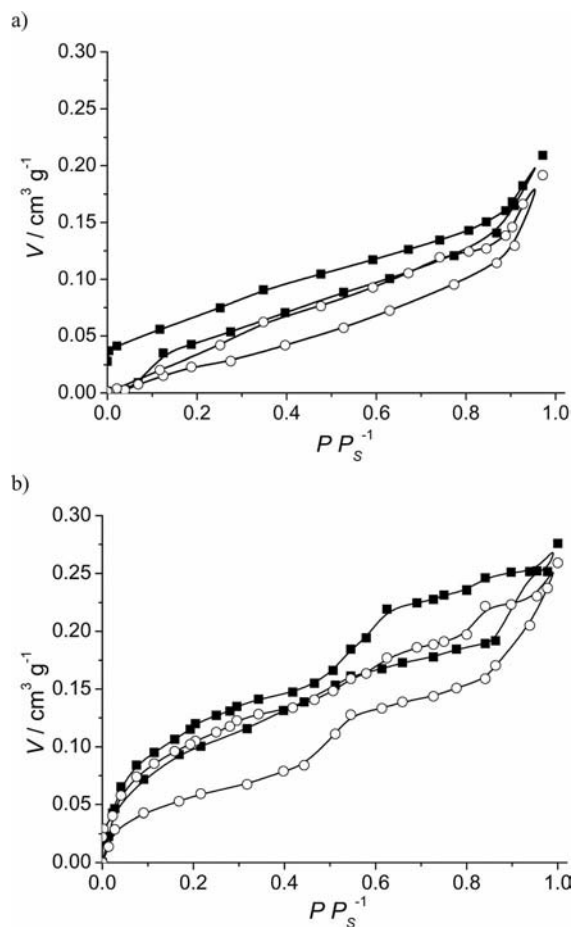


Figure 6. Isotherms of methanol (a) and ethanol (b) sorption by **1** (■) and **2** (○) at 293 K.

Two general conclusions can be made from the results of these sorption experiments. The highest achieved sorption capacity, in terms of pores volume, measured for *n*-octane ($0.25 \text{ cm}^3 \cdot \text{g}^{-1}$) and ethanol ($0.27 \text{ cm}^3 \cdot \text{g}^{-1}$) is higher than the nitrogen sorption capacity at 77 K ($0.22 \text{ cm}^3 \cdot \text{g}^{-1}$) despite the smaller size of the N_2 molecule. This is completely consistent with the conclusions of the X-ray structure determination. As was shown, temperature changes lead to variations in the solvent accessible volume in **1** and **2**. Solvent loss probably leads to a contraction of the pores in **1** and **2**, similar to the change occurring upon cooling which was confirmed by unit cell measurements for the same single crystal over the course of its desolvation. In line with this, the reverse process (pores filling) leads to at least partial “restoration” of the accessible pore volume in the case of sorbates, for which the energy of interaction with structural elements of the coordination polymers (for example E_a , estimated above for alkanes, N_2 and H_2) is sufficient for “expansion” of the structure (at 293 K). When pores are filled by weakly interacting sorbates (N_2 , H_2) and at low temperature (78 K), the sorption capacity is limited by the volume of the “contracted pores”.

The internal surfaces of polymers **1** and **2** are strongly hydrophobic due to the presence of the *tert*-butyl groups of the pivalate residues. This may be favourable for interaction with hydrophobic alkanes but interaction of the same sorbents with hydrophilic alcohols should be weaker. This leads to high (in absolute terms) adsorption energies for alkanes and even at low pressure they fill almost the whole volume of the micropores and can probably cause “expansion” of the pores to their highest possible capacity already at $P/P_S < 0.1$. Continuous growth of the *n*-octane isotherms after “quick” filling of the micropores may be associated with constrictions caused by diffusion of long *n*-octane molecules in the pores. In the case of alcohols, the adsorption energy of these molecules is probably not high enough to fill all the micropores of the coordination polymers at low pressure or to induce rearrangement of the crystal structure thereby leading to pore expansion at low pressure. These substrates seem to fill the pores gradually with increasing pressure and the isotherms do not show saturation in the whole range of P (until the condensation pressure P_S). Even in this case, maximum ethanol sorption capacity is higher than for methanol which is consistent with the expected increase of the contribution of the hydrophobic interactions for alcohols with longer hydrocarbon chains.

Conclusions

In this study we showed that the crystal structures of porous coordination polymers $\text{Fe}_2\text{MO}(\text{Piv})_6(\text{bipy})_{1.5}$ are very flexible in terms of possible rearrangement and this can involve a change of the angle between interpenetrating 2D polymeric layers over a wide range and the distance between the mean planes of such 2D layers. These changes are completely reversible. Both the shape of the pores (channels) and their accessible volume change significantly along with changes in the crystal structures of the compounds. These rearrangements can be induced by different factors such as the nature of the solvent molecules in the pores and the temperature. It was shown that gradual desolvation (evaporation of solvent) from one single crystal at 293 K led to a change of its unit cell parameters and these changes were similar to the change in the unit cell parameters caused by a temperature decrease. Hence, temperature-induced variations in the crystal structure, demonstrated by X-ray structure determination at several temperatures, can model the changes which occur upon desolvation of these compounds. It is very reasonable to suppose that very similar structural rearrangements can be caused by adsorption or desorption of different substrates.

The pores volume, which is accessible in **1** and **2** for *n*-octane and ethanol at 293 K, is higher than the pore volume accessible for N_2 at 78 K. This can be explained by at least partial restoration of the crystal structure after desolvation-induced rearrangement.

A strong difference between the sorption of alkanes and alcohols was found: while alkane (*n*-hexane and *n*-octane)

sorption isotherms were typical for microporous sorbents, adsorption of alcohols (methanol and ethanol) was probably associated with some structural rearrangements, which continuously occur with increasing pressure of the sorbate. This difference, as well as the higher sorption capacity of ethanol compared with that of methanol is consistent with the hydrophobic nature of the channels (due to the presence of multiple *tert*-butyl groups in their structure). In our opinion, the results of the study are important for understanding the possible nature of the “structural flexibility” of porous coordination polymers.

Experimental Section

General: Reagents and solvents were commercially available (Aldrich) and were used without further purification. Compounds $\text{Fe}_2\text{MO}(\text{Piv})_6(\text{bipy})_{1.5} \cdot 2\text{DMF}$ ($\text{M} = \text{Ni}^{\text{II}}$ or Co^{II}) were prepared according to previously reported procedures.^[9] The solvate $\text{Fe}_2\text{NiO}(\text{Piv})_6(\text{bipy})_{1.5} \cdot 2\text{DEF}$ was prepared using a similar procedure^[9] with the only difference being that the reaction was performed in DEF. X-ray structure determinations of all compounds were obtained from data collected from single crystals mounted on a Bruker SMART APEX II diffractometer equipped with a CCD camera and a graphite-monochromated Mo-K_α radiation source ($\lambda = 0.71073 \text{ \AA}$) at various temperatures. Data for **1**·2DMF, collected at 160 K and 260 K, were integrated in the monoclinic crystal system, similarly to previously reported X-ray structures of **1**·2DMF and **2**·2DMF.^[9] In the case of the experiment at 296 K, data for **1**·2DMF were integrated in the orthorhombic crystal system in order to reduce data collection time which was important because of solvent loss. Gradual solvent loss at room temperature in the case of the crystal not covered by silicone oil, led to a gradual change in the unit cell parameters which is described in the section “Temperature- and solvent-induced structure variation of **1**·2Solv and **2**·2Solv”. An effective absorption correction was performed (SCALEPACK). Structures of the complexes were solved with direct method using Sir-97^[13] software and refined with full-matrix least-squares method on F^2 using SHELXL-97.^[14] H atoms were treated by a riding model. Solvent molecules, which could not be localised, were removed by the SQUEEZE procedure (details of structure refinement are presented in Supporting materials).^[10]

CCDC-829631 (for **1**·2DMF at 160 K), -829632 (for **1**·2DMF at 260 K), -829633 (for **1**·2DMF at 296 K), -829634 (for **1**·2DEF at 173 K), -829635 (for **1**·2DEF at 260 K) contain the supplementary crystallographic data for this paper. These data can be obtained free of charge from The Cambridge Crystallographic Data Centre via www.ccdc.cam.ac.uk/data_request/cif.

Thermogravimetric analyses (TGA) were performed in air on a Q1500 instrument. DSC measurements were performed using a NETZSCH 204 F1 instrument in a stream of dry argon ($10 \text{ mL} \cdot \text{min}^{-1}$). Powder X-ray diffraction experiments were performed on a Bruker X9 instrument with Fe radiation ($\lambda = 1.932 \text{ \AA}$). Sorption of *n*-hexane, *n*-octane, methanol and ethanol by **1** and **2** was studied gravimetrically using a quartz microbalance at 293 K. Each point on the absorption and desorption isotherms corresponds to equilibrium conditions (i.e. no change of sample weight at certain $P \cdot P_S^{-1}$, where P_S is the pressure of saturated vapour of the compound at 293 K). In order to remove possible captured molecules from the pores prior to sorption experiments, samples were immersed in acetone for five days which was changed once per day. The samples were then thermally activated at 120°C in vacuo at

10^{-2} Torr. The volume of the pores was estimated from the quantity of adsorbed alkane or alcohol using its density in the liquid phase at 293 K.

Supporting Information (see footnote on the first page of this article): Tables presenting crystal data and structure refinements for **1** and **2**, selected structural features of **1**·2DMF and **2**·2DMF (compounds are isostructural) at different temperatures, unit cell parameters obtained for the same single crystals of **1**·2DMF at room temperature depending on time which correspond to different desolvation levels; figures showing the change of cell parameters for crystals of **1**·2DMF and **2**·2DMF with temperature, change of d and ϕ for **1**·2DMF and **2**·2DMF with temperature, TG curves for **1** and **2**, powder X-ray diffraction patterns for **1**·2DMF, **2**·2DMF as well as solvent-free **1** and **2**, and sorption isotherms (number of coordinated moles of guest per mole of sorbent).

Acknowledgments

Partial funding by the joint grant of the National Academy of Sciences of Ukraine (grant numbers 7/2P and 7/2P-2011) and the Russian Foundation for Basic Research (grant number 10-03-90405), the Council on Grants of the President of the Russian Federation (NSh-3672.2010.3, MK-1185.2011.3), the Russian Academy of Science, and the Ministry of Education and Science of the Russian Federation (GK 14.740.11.0363) are gratefully acknowledged.

- [1] For selected examples, see: a) C. Janiak, J. K. Vieth, *New J. Chem.* **2010**, *34*, 2366–2388; b) S. Kitagawa, R. Kitaura, S. Noro, *Angew. Chem.* **2004**, *116*, 2388; *Angew. Chem. Int. Ed.* **2004**, *43*, 2334–2375; c) U. Mueller, M. Schubert, F. Teich, H. Puetter, K. Schierle-Arndt, J. Pastre, *J. Mater. Chem.* **2006**, *16*, 626–636; d) S. Natarajan, S. Mandal, *Angew. Chem.* **2008**, *120*, 4876; *Angew. Chem. Int. Ed.* **2008**, *47*, 4798–4828; e) L. J. Murray, M. Dincă, J. R. Long, *Chem. Soc. Rev.* **2009**, *38*, 1294–1314.
- [2] For selected examples, see: a) M. Kurmoo, *Chem. Soc. Rev.* **2009**, *38*, 1353–1379; b) D. MasPOCH, D. Ruiz-Molina, J. Veciana, *J. Mater. Chem.* **2004**, *14*, 2713–2723; c) X.-N. Cheng, W.-X. Zhang, Y.-Y. Lin, Y.-Z. Zheng, X.-M. Chen, *Adv. Mater.* **2007**, *19*, 1494–1498; d) D. MasPOCH, D. Ruiz-Molina, J. Veciana, *Chem. Soc. Rev.* **2007**, *36*, 770–818; e) A. S. Lytvynenko, S. V. Kolotilov, O. Cador, K. S. Gavrilenko, S. Golhen, L. Ouahab, V. V. Pavlishchuk, *Dalton Trans.* **2009**, 3503–3509.
- [3] For selected examples, see: a) M. D. Allendorf, C. A. Bauer, R. K. Bhakta, R. J. T. Houk, *Chem. Soc. Rev.* **2009**, *38*, 1330–1352; b) B. V. Harbuzaru, A. Corma, F. Rey, P. Atienzar, J. L. Jordá, H. García, D. Ananias, L. D. Carlos, J. Rocha, *Angew. Chem.* **2008**, *120*, 1096; *Angew. Chem. Int. Ed.* **2008**, *47*, 1080–1083.
- [4] a) Y. Kobayashi, B. Jacobs, M. D. Allendorf, J. R. Long, *Chem. Mater.* **2010**, *22*, 4120–4122; b) M.-H. Zeng, Q.-X. Wang, Y.-X. Tan, S. Hu, H.-X. Zhao, L.-S. Long, M. Kurmoo, *J. Am. Chem. Soc.* **2010**, *132*, 2561–2563; c) M. Sadakiyo, T. Yamada, H. Kitagawa, *J. Am. Chem. Soc.* **2009**, *131*, 9906–9907; d) S. Takaishi, M. Hosoda, T. Kajiwara, H. Miyasaka, M. Yamashita, Y. Nakanishi, Y. Kitagawa, K. Yamaguchi, A. Kobayashi, H. Kitagawa, *Inorg. Chem.* **2009**, *48*, 9048–9050.
- [5] For selected examples, see: a) J.-Y. Lee, O. K. Farha, J. Roberts, K. A. Scheidt, S.-B. T. Nguyen, J. T. Hupp, *Chem. Soc. Rev.* **2009**, *38*, 1450–1459; b) D. Farrusseng, S. Aguado, C. Pinel, *Angew. Chem.* **2009**, *121*, 7638; *Angew. Chem. Int. Ed.* **2009**, *48*, 7502–7513; c) T. Uemura, N. Yanai, S. Kitagawa, *Chem. Soc. Rev.* **2009**, *38*, 1228–1236; d) L. Ma, C. Abney, W. Lin, *Chem. Soc. Rev.* **2009**, *38*, 1248–1256; e) P. K. Thallapally, C. A. Fernandez, R. K. Motkuri, S. K. Nune, J. Liu, C. H. F. Peden, *Dalton Trans.* **2010**, *39*, 1692–1694.
- [6] For selected examples, see: a) R. E. Morris, P. S. Wheatley, *Angew. Chem.* **2008**, *120*, 5044; *Angew. Chem. Int. Ed.* **2008**, *47*, 4966–4981; b) M. Eddaoudi, D. B. Moler, H. Li, B. Chen, T. M. Reineke, M. O’Keeffe, O. M. Yaghi, *Acc. Chem. Res.* **2001**, *34*, 319–330.
- [7] For selected examples, see: a) G. Férey, C. Serre, *Chem. Soc. Rev.* **2009**, *38*, 1380–1399; b) M. Kawano, M. Fujita, *Coord. Chem. Rev.* **2007**, *251*, 2592–2605; c) G. Férey, M. Latroche, C. Serre, F. Millange, T. Loiseau, A. Percheron-Guégan, *Chem. Commun.* **2003**, 2976–2977; d) F. Millange, C. Serre, N. Guilhou, G. Férey, R. I. Walton, *Angew. Chem.* **2008**, *120*, 4168; *Angew. Chem. Int. Ed.* **2008**, *47*, 4100–4105; e) K. Sumida, M. L. Foo, S. Horike, J. R. Long, *Eur. J. Inorg. Chem.* **2010**, 3739–3744; f) T. Loiseau, C. Serre, C. Huguenard, G. Fink, F. Taulelle, M. Henry, T. Bataille, G. Férey, *Chem. Eur. J.* **2004**, *10*, 1373–1382; g) A. Aijaz, P. Lama, P. K. Bharadwaj, *Eur. J. Inorg. Chem.* **2010**, 3829–3834.
- [8] a) H. Chun, J. Seo, *Inorg. Chem.* **2009**, *48*, 9980–9982; b) D. Tanaka, K. Nakagawa, M. Higuchi, S. Horike, Y. Kubota, T. C. Kobayashi, M. Takata, S. Kitagawa, *Angew. Chem.* **2008**, *120*, 3978; *Angew. Chem. Int. Ed.* **2008**, *47*, 3914–3918; c) R. Kitaura, K. Seki, G. Akiyama, S. Kitagawa, *Angew. Chem.* **2003**, *115*, 444; *Angew. Chem. Int. Ed.* **2003**, *42*, 428–431.
- [9] R. A. Polunin, S. V. Kolotilov, M. A. Kiskin, O. Cador, E. A. Mikhalyova, A. S. Lytvynenko, S. Golhen, L. Ouahab, V. I. Ovcharenko, I. L. Eremenko, V. M. Novotortsev, V. V. Pavlishchuk, *Eur. J. Inorg. Chem.* **2010**, 5055–5057.
- [10] A. L. Spek, *Acta Crystallogr., Sect. A* **1990**, *46*, C34.
- [11] I. V. Vasylenko, K. S. Gavrylenko, V. G. Il’yin, V. Golub, G. Goloverda, V. Kolesnichenko, A. W. Addison, V. V. Pavlishchuk, *Mater. Chem. Phys.* **2010**, *121*, 47–52.
- [12] a) K. S. W. Sing, D. H. Everett, R. A. W. Haul, L. Moscou, R. A. Pierotti, J. Rouquerol, T. Siemieniewska, *Pure Appl. Chem.* **1985**, *57*, 603–619; b) S. J. Gregg, K. S. W. Sing, in: *Adsorption, Surface Area and Porosity*, Academic Press, London, **1982**, 2nd ed., p. 4.
- [13] A. Altomare, M. C. Burla, M. Camalli, G. L. Cascarano, C. Giacovazzo, A. Guagliardi, A. G. G. Moliterni, G. Polidori, R. Spagna, *J. Appl. Crystallogr.* **1999**, *32*, 115–119.
- [14] G. M. Sheldrick, *SHELX-97*, University of Göttingen, Germany, **1997**.

Received: July 28, 2011

Published Online: September 22, 2011